Molecular Pharmacology Fast Forward. Published on December 21, 2011 as doi: 10.1124/mol.111.075226
This article has not been copyedited and formatted. The final version may differ from this version.

Characterization of the substituted N-triazole oxindole, TROX-1, a small molecule, state-dependent inhibitor of Ca_V2 calcium channels

Andrew M. Swensen, James Herrington, Randal M. Bugianesi, Ge Dai, Rodolfo J. Haedo, Kevin S. Ratliff, McHardy M. Smith, Vivien A. Warren, Stephen P. Arneric, Cyrus Eduljee, David Parker, Terrance P. Snutch, Scott B. Hoyt, Clare London, Joseph L. Duffy, Gregory J. Kaczorowski, and Owen B. McManus

Department of Ion Channels, Merck Research Laboratories, Rahway, NJ 07065 (A.M.S., J.H., R.M.B., G.D., R.J.H., K.S.R., M.M.S., V.A.W. and O.B.M), Zalicus Pharmaceuticals, Vancouver, BC, Canada (S.P.A., C.E., D.P., T.P.S.) and Department of Medicinal Chemistry, Merck Research Laboratories, Rahway, NJ 07065 (S.B.H., C.L., J.L.D.)

Molecular Pharmacology Fast Forward. Published on December 21, 2011 as DOI: 10.1124/mol.111.075226
This article has not been copyedited and formatted. The final version may differ from this version.

Running title: Characterization of TROX-1, a state-dependent Ca_V2 inhibitor

Corresponding author:

Owen B. McManus

Johns Hopkins Ion Channel Center

Department of Neuroscience

Johns Hopkins School of Medicine

733 North Broadway

Baltimore, MD 21205

443-287-4410

410-614-1001 (FAX)

owen_mcmanus@jhmi.edu

Number of text pages: 25

Number of tables: 1

Number of figures: 7

Number of references: 40

Number of words in Abstract: 250

Number of words in Introduction: 592

Number of words in Discussion: 1466

Non-standard Abbreviations: bMHN-4, CBK, and 2H8, $Ca_v2.2$ HEK cell lines; Ca_v, voltage-gated calcium channel; DMSO, dimethyl sulfoxide; GVIA, ω-conotoxin GVIA;. TROX-1, (3*R*)-5-(3-chloro-4-fluorophenyl)-3-methyl-3-(pyrimidin-5-ylmethyl)-1-(1*H*-1,2,4-triazol-3-yl)-1,3-dihydro-2*H*-indol-2-one.

Molecular Pharmacology Fast Forward. Published on December 21, 2011 as DOI: 10.1124/mol.111.075226
This article has not been copyedited and formatted. The final version may differ from this version.

Abstract

Biological, genetic, and clinical evidence provide validation for N-type calcium channels ($Ca_V2.2$) as therapeutic targets for chronic pain. A state-dependent $Ca_V2.2$ inhibitor may provide an improved therapeutic window over ziconotide, the peptidyl $Ca_V2.2$ inhibitor used clinically. Supporting this notion, we recently reported that the state-dependent Ca_V2 inhibitor TROX-1 has an improved therapeutic window compared to ziconotide in preclinical models. Here we characterize TROX-1 inhibition of Cav2.2 channels in more detail. When channels are biased towards open/inactivated states by depolarizing the membrane potential under voltage-clamp electrophysiology, TROX-1 inhibits $Ca_V2.2$ channels with an IC_{50} of 0.11 μM. The voltage-dependence of $Ca_V2.2$ inhibition was examined using automated electrophysiology. TROX-1 IC_{50} values were 4.2 μM at -110 mV, 0.90 μM at -90 mV, and 0.36 μM at -70 mV. TROX-1 displayed use-dependent inhibition of $Ca_V2.2$ with a 10-fold IC_{50} separation between first (27 μM) and last (2.7 μM) pulses in a train. In a fluorescence-based calcium influx assay, TROX-1 inhibited $Ca_V2.2$ channels with an IC_{50} of 9.5 μM under hyperpolarized conditions and 0.69 μM under depolarized conditions. Lastly, TROX-1 potency was examined across the Ca_V2 subfamily. Depolarized IC_{50} values were 0.29 μM, 0.19 μM and 0.28 μM by manual electrophysiology using matched conditions and 1.8 μM, 0.69 μM and 1.1 μM by calcium influx for $Ca_V2.1$, $Ca_V2.2$ and $Ca_V2.3$, respectively. Together, these in-vitro data support the idea that a state-dependent, non-subtype selective Ca_V2 channel inhibitor can achieve an improved therapeutic window over the relatively state-*independent*, $Ca_V2.2$-selective inhibitor ziconotide in preclinical models of chronic pain.

Molecular Pharmacology Fast Forward. Published on December 21, 2011 as DOI: 10.1124/mol.111.075226
This article has not been copyedited and formatted. The final version may differ from this version.

Introduction

The Ca_V2 subfamily of voltage-dependent calcium channels serves a critical role in the nervous system. This subfamily consists of $Ca_V2.1$ (P/Q-type), $Ca_V2.2$ (N-type) and $Ca_V2.3$ (R-type) channels. These calcium channels provide the main pathway for voltage-triggered calcium influx and subsequent neurotransmitter release at many synapses. Although all three subfamily members likely contribute to processing nociceptive inputs (Pietrobon, 2005), most drug discovery efforts seeking treatments for pathological pain have focused on the $Ca_V2.2$ subtype (Yamamoto and Takahara, 2009).

There is extensive evidence to support $Ca_V2.2$ as a target for chronic pain treatment. $Ca_V2.2$ channels are highly expressed in laminae I and II of the spinal cord (Gohil et al., 1994; Westenbroek et al., 1998) and are up-regulated in behavioral pain models (Abbadie et al., 2010; Cizkova et al., 2002). Laminae I and II serve as critical relay points in the transmission of pain information into the CNS, where primary nociceptors make synaptic connections with dorsal horn neurons of the spinal cord. Opening of presynaptic $Ca_V2.2$ channels in response to depolarization of the primary afferent terminal triggers release of transmitter into the synaptic cleft (Evans et al., 1996). Blocking these $Ca_V2.2$ channels with conopeptides attenuates nociception in behavioral models of neuropathic and inflammatory pain (Malmberg and Yaksh, 1995; Scott et al., 2002). Furthermore, $Ca_V2.2$ knockout mice display reduced pain sensitivity in a number of pain models (Abbadie et al., 2010; Hatakeyama et al., 2001; Kim et al., 2001; Saegusa et al., 2001). Perhaps most convincing are the clinical data from ziconotide, a selective peptide blocker of $Ca_V2.2$ channels, which is efficacious in the treatment of chronic pain (Miljanich, 2004).

Molecular Pharmacology Fast Forward. Published on December 21, 2011 as DOI: 10.1124/mol.111.075226
This article has not been copyedited and formatted. The final version may differ from this version.

While ziconotide provides efficacy against chronic pain its use is limited by its small therapeutic window and intrathecal route of administration (Miljanich, 2004; Staats et al., 2004). Although some state-dependence to ziconotide block is revealed at very negative potentials, within physiological voltage ranges ziconotide potently inhibits $Ca_V2.2$ channels regardless of whether they are in the open, closed, or inactivated state (Feng et al., 2003; Stocker et al., 1997). Small molecule inhibitors demonstrating strong state-dependent inhibition have been well described for L-type and T-type calcium channels (e.g. (Bean, 1984; McDonough and Bean, 1998) and it has been proposed that a state-dependent $Ca_V2.2$ inhibitor, which preferentially binds to channels in open or inactivated states, may provide efficacy with an improved therapeutic window over ziconotide due to enhanced activation of $Ca_V2.2$ channels in pain conditions (McGivern and McDonough, 2004; Snutch, 2005; Winquist et al., 2005). A number of small molecule $Ca_V2.2$ inhibitors have been described in the literature (reviewed in Yamamoto and Takahara, 2009), although detailed mechanistic characterizations of these compounds have not been reported, preventing determination of the value of state-dependent inhibitors in pain treatment.

TROX-1, a substituted N-triazole oxindole, is a $Ca_V2.2$ inhibitor which exhibits efficacy in a number of animal pain models with a therapeutic window for both cardiovascular and CNS side effects (Abbadie et al., 2010). Here we show electrophysiologically that TROX-1 inhibits $Ca_V2.2$ channels in both a state-dependent and use-dependent manner. Since state-dependent calcium channel inhibitors can exhibit apparent subtype selectivity due to different levels of channel inactivation across channel subtypes, we measured the activity of TROX-1 on members of the Ca_V2 subfamily at

Molecular Pharmacology Fast Forward. Published on December 21, 2011 as DOI: 10.1124/mol.111.075226
This article has not been copyedited and formatted. The final version may differ from this version.

various levels of inactivation. When the differences in inactivation are accounted for, TROX-1 is shown to have little molecular subtype selectivity within the Ca_V2 subfamily. Nevertheless, these results suggest that 'functional' selectivity may still be obtained over Ca_V2 channel isoforms which have more depolarized inactivation-voltage relationships or Ca_V2 channels that are expressed in cells with more hyperpolarized resting potentials.

Molecular Pharmacology Fast Forward. Published on December 21, 2011 as DOI: 10.1124/mol.111.075226
This article has not been copyedited and formatted. The final version may differ from this version.

Materials and Methods

Chemicals

TROX-1 ((3R)-5-(3-chloro-4-fluorophenyl)-3-methyl-3-(pyrimidin-5-ylmethyl)-1-(1H-1,2,4-triazol-3-yl)-1,3-dihydro-2H-indol-2-one) was synthesized at Merck Research Labs, Rahway, NJ. Stock solutions of TROX-1 were prepared in DMSO at 10 mM and diluted into assay buffer solutions immediately prior to use. ω-Conotoxin GVIA was obtained from Sigma-Aldrich (St. Louis, MO).

Cell lines and growth conditions

Stable HEK293 cell lines expressing human Ca_V2 calcium channels were previously described (Dai et al., 2008). The $Ca_V2.1$ stable line expressed the α1A-2 (P-type) splice variant (Hans et al., 1999). The $Ca_V2.2$ cell lines (2H8 and CBK) utilized the long form of α1B-1 (Williams et al., 1992). For $Ca_V2.3$, the α1E-3 splice variant was used (Williams et al., 1994). Each cell line expressed α2bδ-1 and β3a auxiliary subunits (Williams et al., 1992). Following creation of the stable cell lines expressing calcium channels, each line was transfected with cDNA encoding human Kir2.3 (KCNJ4) (Perier et al., 1994) and clonal selection was performed. For electrophysiological experiments, an additional $Ca_V2.2$ cell line (bMHN-4) was produced that afforded increased expression levels and improved performance in electrophysiological assays. HEK-293 cells were transfected using a dual vector approach, pcDNA3.1 with long form α1B-1 and pBudCE4 with α2δ-1 and β3. Clones were selected based on $Ca_V2.2$ channel expression using ^{125}I-ω-CgTx-GVIA binding levels and high-expressing clones were further characterized in electrophysiological experiments. Cell lines were cultured at 37 °C in DMEM (Cellgro #10-013-CM) supplemented with 10% fetal bovine serum

Molecular Pharmacology Fast Forward. Published on December 21, 2011 as DOI: 10.1124/mol.111.075226
This article has not been copyedited and formatted. The final version may differ from this version.

(Invitrogen/Gibco #16000-036), penicillin, streptomycin, and glutamine additive (Invitrogen/Gibco #10378-016) and appropriate selection antibiotics. $Ca_V2.1$ and $Ca_V2.3$ cell lines were maintained at 5% CO_2; $Ca_V2.2$ cells were maintained at 10% CO_2. $Ca_V2.2$ and $Ca_V2.3$ cell lines were maintained at 30 °C for one day and $Ca_V2.1$ cells for two to three days prior to use to enhance expression levels.

Manual Electrophysiology

Membrane currents were recorded from the stable HEK293 recombinant cell lines expressing either $Ca_V2.1$, $Ca_V2.2$ (bMHN-4 cell line), or $Ca_V2.3$ channels using the whole-cell patch clamp technique with a HEKA (Port Washington, NY) EPC 10 patch-clamp or an Axopatch 200B patch-clamp amplifier. Fire-polished borosilicate glass electrodes had resistances from 1-3 MΩ when filled with internal solution. Solutions were applied to cells by bath perfusion via gravity and flow of solution through the chamber was maintained at all times. Cells exhibiting stable current amplitudes were challenged with compound dissolved in DMSO such that the final DMSO concentration typically did not exceed 0.1% of the external solution and did not affect assay results. For experiments testing the effects of 30 μM TROX-1, control and compound solutions had a final DMSO concentration of 0.3%. Compounds were added in escalating concentrations for a minimum of 4 minutes and percent inhibition was measured after steady state inhibition was achieved at each concentration. IC_{50} values for Ca_V inhibition were calculated from the fits to the Hill equation (Percent Inhibition = 100*(1/(1+(IC_{50}/[Compound])^n_H)) with the slope, n_H, fixed to 1. For the initial manual electrophysiology experiments (Figures 1 and 2), bMHN-4 cells were grown on poly-D-

Molecular Pharmacology Fast Forward. Published on December 21, 2011 as DOI: 10.1124/mol.111.075226
This article has not been copyedited and formatted. The final version may differ from this version.

lysine coated coverglass. The extracellular solution contained (in mM): 5 $BaCl_2$, 139 CsCl, 1 $MgCl_2$, 10 HEPES, 10 glucose, 10 sucrose, pH adjusted to 7.4 with CsOH. The intracellular solution contained (in mM): 126.5 Cs-methanesulfonate, 2 Mg Cl_2, 11 EGTA, 10 HEPES, 2 Na_2-ATP; osmolarity was adjusted to 295 mOsm using sucrose and pH to 7.3 using CsOH. Leak subtraction was performed using a P/4 protocol. The purpose in some manual electrophysiology experiments was to compare inhibition of $Ca_V2.2$ channels with inhibition of $Ca_V2.1$ and $Ca_V2.3$ channels (Figure 5). Due to differences in growth patterns between the three cell lines, cells were acutely dissociated from T25 flasks before use. To compensate for lower channel expression levels in the $Ca_V2.1$ and $Ca_V2.3$ cell lines, a 20 mM barium external solution containing (in mM): 120 NaCl, 20 $BaCl_2$, 4.5 KCl, 0.5 $MgCl_2$, 10 HEPES, 10 glucose, pH 7.4 with NaOH, was utilized for all three cell lines in these experiments. The internal solution for these experiments contained (in mM): 130 CsCl, 10 EGTA, 10 HEPES, 2 $MgCl_2$, 3 MgATP, pH 7.3 with CsOH.

For generating the current versus voltage relationship for the bMHN-4 line, cells were voltage-clamped at -100 mV and peak currents measured during 15 ms voltage steps ranging from -65 mV to +50 mV in 5 mV increments. Following each step, cells were stepped back down to -50 mV where deactivation was slow enough to measure tail currents. Normalized tail current measurements were used for generating the activation curve. For the inactivation protocol, cells were voltage-clamped at -110 mV and stepped to voltages ranging from -130 to -10 mV for 10 seconds (prepulses), and then to +10 mV to elicit current through non-inactivated channels. Sweeps were repeated every 40 seconds. Control currents were elicited before each prepulse to assure that there was not

substantial rundown and that the currents were sufficiently recovered from the previous prepulse. Resulting data were fit to a Boltzmann function: $y = 1/(1+\exp((V_h-V) / k))$, where y is the current normalized with respect to the maximal current, V_h is the voltage at which half activation or inactivation is reached, V is the voltage, and k is the slope factor. Data are reported as the mean ± S.E.M.

Automated Electrophysiology using PatchXpress

PatchXpress™ is a 16-well whole-cell automated patch clamp device that operates asynchronously with fully integrated fluidics (Molecular Devices Corp, Sunnyvale, CA). For PatchXpress™ experiments, cells were grown in T75 culture flasks and dissociated with trypsin 30-60 minutes before use. Capacitance and series resistance compensation were automatically applied and no correction for liquid junction potentials was employed. Leak subtraction was performed using the P/N procedure. Voltage protocols and the recording of membrane currents were performed using the PatchXpress™ software/hardware system and current amplitudes were calculated with DataXpress™ software. In order to increase current amplitudes and assay reliability, the same 20 mM barium external solution and corresponding internal solution used for the manual electrophysiology experiments were also used for the PatchXpress™ experiments. The bMHN-4 cell line was used for the state-dependent assay and the CBK cell line was used for the use-dependent assay. Compounds were added in escalating concentrations (0.3 μM to 30 μM) using an integrated pipettor from a 96-well compound plate. Percent inhibition of peak current by TROX-1 was calculated from the ratio of the current amplitude in the presence and absence of compound. Data are reported as the mean ±

Molecular Pharmacology Fast Forward. Published on December 21, 2011 as DOI: 10.1124/mol.111.075226
This article has not been copyedited and formatted. The final version may differ from this version.

S.E.M. IC_{50} values for $Ca_V2.2$ inhibition were calculated from fits of the Hill equation with the slope fixed to 1.

$Ca_V2.x$ Channel Calcium Influx Assays

Fluorescence-based calcium influx assays as described in Dai et al. (2008) were used to characterize the effects of TROX-1 on $Ca_V2.x$ channels. Expression of Kir2.3 channels in each cell line allowed control of cell membrane potential through changes in bath potassium concentration (Dai et al., 2008). TROX-1 was incubated with each cell line in the presence of varying levels of bath potassium concentration to assess channel inhibition at different membrane potentials and levels of channel inactivation. After 30 minutes compound incubation, channel opening was initiated by 1:1 addition of buffer solution containing 140 mM potassium. Calcium influx signals were measured using a 384 well FLIPR Tetra™ (Molecular Devices Corp, Sunnyvale, CA) and calcium indicator dye (Fluo-4). The assay protocol is described below. Cells were seeded in poly-D-lysine coated 384-well plates and kept in an incubator overnight at 30 °C for $Ca_V2.2$ and $Ca_V2.3$ cell lines and at 30 °C for two to three days for $Ca_V2.1$ cells. Media was removed and cells were washed with 50 µl Dulbecco's Phosphate Buffered Saline (D-PBS) with calcium & magnesium (Invitrogen; 14040). Fifty µl of 4 µM Fluo-4 (Molecular Probes; F-14202) and 0.02% pluronic acid (Molecular Probes; P-3000) prepared in D-PBS supplemented with 10 mM glucose & 10 mM HEPES/NaOH; pH 7.4 was added to each well. Cells were incubated in the dark at 25 °C for 60-70 min. Dye was removed and cells were washed with 60 µl of Potassium Pre-polarization Buffer. (PPB (in mM)**:** x KCl, 150-x NaCl, 0.8 $CaCl_2$, 1.7 $MgCl_2$, 10 HEPES, pH=7.2). Thirty µl of PPB was added to each well with or without test compound and cells were

Molecular Pharmacology Fast Forward. Published on December 21, 2011 as DOI: 10.1124/mol.111.075226
This article has not been copyedited and formatted. The final version may differ from this version.

incubated in the dark at 25 °C for 30 min. Fluorescence intensity was measured on a FLIPR Tetra™ instrument (excitation = 480 nm, emission = 535 nm). While continuously reading fluorescence intensity for 40 s, 30 µl of Depolarization Buffer (in mM): 140 KCl, 10 NaCl, 0.8 $CaCl_2$, 1.7 $MgCl_2$, 10 HEPES, pH=7.2, which is 2x the final assay concentration, was added to each well after 10 s. Peak fluorescent signal intensity was determined and the amplitude of the peak signal, normalized to baseline, was used to measure channel inhibition by test compounds. Data are reported as the mean ± S.E.M. IC_{50} values for $Ca_V2.x$ inhibition were calculated from fits of the Hill equation to the titration data.

Molecular Pharmacology Fast Forward. Published on December 21, 2011 as DOI: 10.1124/mol.111.075226
This article has not been copyedited and formatted. The final version may differ from this version.

Results

Characterization of $Ca_V2.2$ cell lines

The $Ca_V2.2$ (2H8) cell line used in the calcium influx assay and the $Ca_V2.1$ and $Ca_V2.3$ cell lines used in both the electrophysiological and influx assays were previously characterized (Dai et al., 2008). For electrophysiological studies involving $Ca_V2.2$, a new cell line was created with improved current stability. New cell lines were created using a dual vector approach (see Materials and Methods). Clones with high $Ca_V2.2$ expression were initially selected using an ^{125}I-ω-CgTx-GVIA binding assay and then characterized electrophysiologically on the PatchXpress™, an automated patch clamp platform, to select clones with high functional expression, appropriate biophysical properties, and favorable current stability over time. Using these criteria, the bMHN-4 clone was selected for electrophysiological experiments. The current expressed in the bMHN-4 cell line was larger than that in the original CBK line and, although smaller than that expressed in the 2H8 cell line, was more stable over time (Table 1, Fig. 1A). The bMHN-4 cell line was characterized in more detail by conventional electrophysiology. Maximal current was elicited at ~ +5 mV with half activation occurring at +4 mV and half inactivation at -80 mV (Fig. 1B). Addition of 500 nM of the $Ca_V2.2$-selective peptide inhibitor, ω-conotoxin-GVIA, inhibited 99% of the current elicited from voltage steps to +10 mV (n=3 cells; Fig. 1C).

TROX-1 inhibits $Ca_V2.2$ currents in a voltage- and use-dependent manner

State-dependent inhibition of $Ca_V2.2$ channels by TROX-1 was evaluated by applying the compound at two different membrane potentials using the bMHN-4 recombinant cell line.

Molecular Pharmacology Fast Forward. Published on December 21, 2011 as DOI: 10.1124/mol.111.075226
This article has not been copyedited and formatted. The final version may differ from this version.

Closed state inhibition was estimated during TROX-1 application at a hyperpolarized membrane potential (-115 mV), where channels are biased towards the closed-state; the level of channel inhibition was determined during 20 ms voltage steps to +10 mV every 30 seconds to elicit current through available, unblocked channels. Potential inhibition of inactivated and/or open channels was explored by applying TROX-1 at more depolarized membrane potentials with approximately 30% apparent channel inactivation (-75 mV to -85 mV). Peak currents were measured during 50 ms voltage steps to +10 mV every 15 seconds. For both hyperpolarized and depolarized voltage formats, after stable baseline currents were obtained, compounds were applied by bath perfusion until steady-state inhibition was achieved. Representative current traces for $Ca_V2.2$, +/- 300 nM TROX-1, are shown for the depolarized (Fig. 2B) and the hyperpolarized (Fig. 2C) assay formats. Using the depolarized protocol, TROX-1 inhibited $Ca_V2.2$ in a concentration-dependent manner with an estimated IC_{50} of 0.11 μM (Fig. 2D). Under hyperpolarized conditions, where channels are biased towards the closed state, TROX-1 was less potent, blocking only 14 ± 6% and 45 ± 7 % of the calcium current at 0.3 μM and 3 μM, respectively .

The dependence of TROX-1 activity on membrane potential and channel state was further characterized using PatchXpress™. As for the manual patch clamp assay, cells were stepped to +10 mV every 15 seconds to elicit current and evaluate inhibition. The holding potential, however, was varied in 20 mV increments from -110 mV to –70 mV for different groups of cells. Representative current versus time plots and current traces are shown for TROX-1 inhibition of $Ca_V2.2$ from a holding potential of -70 mV (Fig. 3A) and -110 mV (Fig. 3B). Similar to the results for manual patch assay, the apparent

Molecular Pharmacology Fast Forward. Published on December 21, 2011 as DOI: 10.1124/mol.111.075226
This article has not been copyedited and formatted. The final version may differ from this version.

potency of TROX-1 depended on the holding membrane potential with the IC_{50} shifting from 0.36 μM at -70 mV to 4.2 μM at -110 mV (Fig. 3C).

Use-dependent inhibition of $Ca_V2.2$ channels expressed in the CBK cell line was examined using PatchXpress™. The CBK cell line was chosen because the currents in response to voltage trains were more stable than the currents in 2H8 or bMHN-14 cells. The cause of these stability differences is unclear but may involve differences in channel inactivation across the cell lines. The $Ca_V2.2$ currents in CBK cells exhibit a more depolarized, two component steady-state inactivation curve probably due to limiting expression of β3a (discussed in Dai et al., 2008). CBK cells were voltage clamped at –60 mV, which corresponds to ~80% availability at steady-state, and trains of 20 pulses (25 ms) to +20 mV were applied at a frequency of 2 Hz every 5 minutes. Representative currents at pulse 1 and pulse 20 under control conditions and in the presence of 3 μM TROX-1 are shown in Fig. 4A. Inspection of the time course of current reduction during the pulse train shows that inhibition mainly develops over the first 10 pulses and has reached steady-state by the 20th pulse (Fig. 4C). The averaged data presented in Fig. 4B illustrates that TROX-1 inhibited the current elicited at pulse 20 more potently (IC_{50} = 2.4 μM) than the current elicited at pulse 1 (IC_{50} = 24 μM) indicating enhanced inhibition of $Ca_V2.2$ channels after a train of depolarizing pulses that open and inactivate $Ca_V2.2$ channels.

Together, these data demonstrate TROX-1 inhibits $Ca_V2.2$ channels in both a voltage- and use-dependent manner and are consistent with state-dependent inhibition of inactivated and/or open channels by TROX-1.

Molecular Pharmacology Fast Forward. Published on December 21, 2011 as DOI: 10.1124/mol.111.075226
This article has not been copyedited and formatted. The final version may differ from this version.

TROX-1 inhibits other members of the Ca_V2 subfamily of calcium channels

In manual electrophysiology experiments TROX-1 activity was compared across other members of the Ca_V2 subfamily of calcium channels to assess its selectivity profile. Lower expression levels in the $Ca_V2.1$ and $Ca_V2.3$ cell lines required an increase in the concentration of the barium charge carrier from 5 mM (Fig. 2) to 20 mM. TROX-1 activity on $Ca_V2.2$ was re-assessed using 20 mM barium as the charge carrier to allow for a direct comparison of potency across all three Ca_V2 subfamily members without concern for potency shifts that might result from differences in the concentration of the charge carrier. TROX-1 inhibition of Ca_V2 currents was measured using both 'hyperpolarized' and 'depolarized' voltage formats as described previously (Dai et al., 2008). In brief, for the hyperpolarized format, cells were voltage-clamped at -100 mV and stepped to +10 mV every 15 seconds. For the depolarized format, cells were also stepped to +10 mV every 15 seconds, however, cells were first voltage-clamped at -100 mV to establish a baseline current amplitude and then depolarized to a holding membrane potential which resulted in ~ 30% inactivation of the current. For $Ca_V2.2$ and Ca_V 2.3 channels this voltage was typically -70 to -75 mV. For the less inactivating $Ca_V2.1$ cell line, this voltage was ~ -40 mV. Under the hyperpolarized conditions, TROX-1 showed an apparent selectivity for $Ca_V2.2$ and $Ca_V2.3$ over $Ca_V2.1$ (Fig. 5, squares: IC_{50} = 37 μM for $Ca_V2.1$, 1.1 μM for $Ca_V2.2$, and 1.2 μM for $Ca_V2.3$). However, when TROX-1 inhibition of Ca_V2 channels was assessed under depolarized conditions where the channels exhibited similar levels of inactivation, no selectivity was apparent (Fig. 5, circles: IC_{50} = 0.29 μM for $Ca_V2.1$, 0.19 μM for $Ca_V2.2$, and 0.28 μM for $Ca_V2.3$).

Molecular Pharmacology Fast Forward. Published on December 21, 2011 as DOI: 10.1124/mol.111.075226
This article has not been copyedited and formatted. The final version may differ from this version.

TROX-1 inhibition of Ca_V2 channels was also examined in a calcium influx assay on a FLIPR™ with the throughput to assess inhibition of all three subfamily members across a range of conditions (see Dai et al., 2008). This assay utilizes $Ca_V2.1$, $Ca_V2.2$ and $Ca_V2.3$ cell lines which co-express the Kir2.3 inward rectifier potassium current and therefore allows the membrane potential of the cells to be varied by changing the external potassium concentration. Cells were pre-incubated in potassium pre-polarization buffers with variable potassium concentrations, +/- TROX-1, and then channel opening triggered with a high K^+ depolarization buffer (see Methods). Figure 6 compares TROX-1 inhibition of calcium influx when the pre-incubation external potassium was relatively low (A, 4 mM), and when the external potassium was higher (B, 14 mM). The top section of each subpanel in Fig. 6 shows example calcium influx data from a row of twenty four wells in a 384 well assay plate. The leftmost two wells in each row contain a positive toxin control followed by two wells containing control buffer and the remaining wells containing increasing concentrations of TROX-1 in duplicate. Analysis of concentration-response data are shown in the bottom section of each subpanel. Using these potassium concentrations, $Ca_V2.2$ and $Ca_V2.3$ channels show a marked shift in TROX-1 potency between the 4 mM K^+ and 14 mM K^+ conditions (IC_{50} values decreasing from 9.48 μM to 0.69 μM for $Ca_V2.2$ and 5.13 μM to 1.09 μM for $Ca_V2.3$), while the shift for $Ca_V2.1$ channels was more moderate (IC_{50} decreased from 25.6 μM to 12.4 μM). A large part of this differential shift between the Ca_V2 subfamily members is a result of the weaker potency of TROX-1 on $Ca_V2.1$, relative to $Ca_V2.2$ and $Ca_V2.3$, under the 14 mM K^+ condition. Although the three cells lines should be at similar voltages in 14 mM K^+ (Dai et al., 2008), the fluorescence values from Fig. 6 show that the calcium

Molecular Pharmacology Fast Forward. Published on December 21, 2011 as DOI: 10.1124/mol.111.075226
This article has not been copyedited and formatted. The final version may differ from this version.

influx for $Ca_V2.2$ and $Ca_V2.3$ is reduced in the 14 mM K^+ condition but relatively unchanged for $Ca_V2.1$. This is consistent with the more depolarized inactivation-voltage relationship of $Ca_V2.1$ relative to $Ca_V2.2$ and $Ca_V2.3$ (see Fig. 1B and Dai et al., 2008, Fig. 2D).

To better understand the relationship between calcium channel inactivation and potency, TROX-1 inhibition of $Ca_V2.1$, $Ca_V2.2$ and $Ca_V2.3$-mediated calcium influx was examined across a range of external potassium concentrations. The dependency of the calcium signal on external potassium varied across the three Ca_V2 subfamily members with $Ca_V2.1$ being the most right shifted (Fig. 7A-C, black hollow squares). Similarly, the dependency of TROX-1 potency on external potassium varied across the three subfamily members with $Ca_V2.1$ again being the most right-shifted (Fig.7A-C, colored open symbols). Interestingly, if the IC_{50} for TROX-1 inhibition is plotted versus the fractional reduction in calcium signal, there is little difference in the potency of TROX-1 across the three Ca_V2 subfamily members (Fig. 7D). These results suggest that the apparent differences in TROX-1 potencies observed under different assay conditions are simply a reflection of the degree of inactivation between the channels. Taken together, these data show that TROX-1 is a highly state-dependent inhibitor of all three members of the Ca_V2 subfamily of calcium channels with very little, if any, true molecular selectivity across subtypes.

Molecular Pharmacology Fast Forward. Published on December 21, 2011 as DOI: 10.1124/mol.111.075226
This article has not been copyedited and formatted. The final version may differ from this version.

Discussion

The results reported here show that the substituted N-triazole oxindole, TROX-1, is a potent state-dependent inhibitor of human $Ca_V2.2$ calcium channels. Measured electrophysiologically under depolarized conditions, TROX-1 inhibits recombinant $hCa_V2.2$ currents with an estimated IC_{50} of 0.11 μM. However, when cells are hyperpolarized to minimize open and inactivated state inhibition, TROX-1 potency is reduced, blocking only 45 ± 7% of the current at 3 μM. These results are in good agreement with IC_{50} values for TROX-1 inhibition of native calcium channel currents from dissociated rat DRG neurons under depolarized (0.4 μM) and hyperpolarized (μM) conditions (Abbadie et al., 2010). The state-dependence of TROX-1 inhibition of calcium channels was also observed using a calcium influx assay where the TROX-1 IC_{50} shifted from 0.69 μM under high external potassium (14 mM K^+, partially inactivated) conditions to 9.48 μM under low external potassium (4 mM K^+) conditions. This is in reasonable agreement with the 0.27 μM and >10 μM values from Abbadie et al. (2010) which were obtained using a different cell line and with 30 mM K^+ for the high potassium condition. Electrophysiologically, TROX-1 also inhibited $Ca_V2.2$ channels in a use-dependent manner. TROX-1 inhibited $Ca_V2.2$ current during the 20^{th} pulse of a 2 Hz train approximately 10-fold more potently then during the 1^{st} pulse of the train.

Since TROX-1 shows selectivity for $Ca_V2.2$ over $Ca_V1.2$ (L-type, 18 μM) and $Ca_V3.1/3.2$ (T-type, 15 μM and > 20 μM, respectively) (Abbadie et al., 2010) we also wanted to determine TROX-1 selectivity within the Ca_V2 subfamily. Electrophysiologically, when cells are depolarized to obtain comparable levels of inactivation, TROX-1 has a similar potency across $Ca_V2.1$, $Ca_V2.2$ and $Ca_V2.3$ calcium

Molecular Pharmacology Fast Forward. Published on December 21, 2011 as DOI: 10.1124/mol.111.075226
This article has not been copyedited and formatted. The final version may differ from this version.

channels. However, when cells are voltage-clamped at -100 mV, TROX-1 appears >30-fold selective for $Ca_V2.2$ and $Ca_V2.3$ relative to $Ca_V2.1$. Interestingly, while -100 mV is near the foot of the inactivation curve for both $Ca_V2.2$ and $Ca_V2.3$, it is ~60 mV hyperpolarized from the foot of the inactivation curve for $Ca_V2.1$ (see Fig 1B and Dai et al. (2008) Fig. 2D). The apparent difference in potency, therefore, may reflect the fact that the $Ca_V2.1$ potency at -100 mV better approximates closed-state inhibition. The results from the calcium influx experiments support this interpretation. In the calcium influx assays, the relationship between IC_{50} and external potassium is shifted to higher potassium concentrations (more depolarized) for $Ca_V2.1$ relative to $Ca_V2.2$ and $Ca_V2.3$ (Fig. 7A-C). If, however, IC_{50} values are plotted versus fractional reduction in calcium signal to normalize for channel inactivation, TROX-1 potency is essentially identical for $Ca_V2.1$, $Ca_V2.2$ and $Ca_V2.3$ across a range of inactivation levels (Fig. 7D). These results suggest that TROX-1 is interacting with the inactivated state of the channel, although these data do not exclude other potential mechanisms such as effects on open channels, channel activation, or closed-closed channel state transitions the might occur at depolarized potentials. While these results indicate that there may be little true molecular selectivity within the Ca_V2 subfamily, TROX-1 could still be functionally selective against less inactivated Ca_V2 calcium channels. This is likely a physiologically relevant consideration as Ca_V2 inactivation levels are not only modulated by the voltage and activity of the neurons expressing them, but also can be dependent on the splice variant (Bourinet et al., 1999; Thaler et al., 2004), co-expressed auxiliary subunit (De Waard and Campbell, 1995), or interacting proteins including synaptic proteins (Bezprozvanny et al., 1995; Kiyonaka et al., 2007; Zhong et al., 1999)

Molecular Pharmacology Fast Forward. Published on December 21, 2011 as DOI: 10.1124/mol.111.075226
This article has not been copyedited and formatted. The final version may differ from this version.

Molecular selectivity can be examined in both the electrophysiological and calcium influx assays by measuring potency under similar levels of inactivation (see also Dai et al., 2008), however, more caution should be taken when comparing the absolute degree of state-dependence across the different Ca_V2 assays. The degree of state-dependence is determined by comparing the potency under depolarized conditions to the potency under hyperpolarized conditions where channels are presumed to be largely in the closed-state. However, as discussed above for the electrophysiological assay, the potency values in the calcium influx assay under hyperpolarized conditions (low potassium) are likely influenced by the proximity of the cell resting potential to the foot of the inactivation curve. $Ca_V2.1$ and $Ca_V2.2$ channels appear largely non-inactivated at 4 mM extracellular K^+ in these cell lines since the top of the inactivation curves are relatively flat (Figs. 7A,B). The decreasing signal for $Ca_V2.3$, however, suggests that it is close to the foot of its inactivation curve and this may contribute to its slightly increased potency in 4 mM K^+ (Fig. 7C) and, therefore, its reduced apparent state-dependence. As a result, the state-dependent measures from these assays are most useful for comparing different compounds on the same channel rather than the same compound across different channels.

There is a tendency for TROX-1 to appear more potent in the electrophysiological assays. This is consistent with that reported for two other $Ca_V2.2$ inhibitors assessed in these same assays (Dai et al., 2008) and may be tied to differences between the assay formats. While the cell membrane potentials in the calcium influx assay are likely to be relatively constant during compound incubation, the cells are depolarized periodically in

the electrophysiological assay which could contribute an additional use-dependent component to the inhibition.

The issue of selectivity within the Ca_V2 subfamily of calcium channels raises the question- how might the individual inhibitory activities on $Ca_V2.1$, $Ca_V2.2$, and $Ca_V2.3$ influence overall efficacy and safety profiles? Genetic ablation of these channels in mice likely only provides a partial answer. $Ca_V2.3^{-/-}$ mice, for example, have been reported to be resistant to inflammatory pain but otherwise exhibit a predominantly normal phenotype with alterations in glucose metabolism (Matsuda et al., 2001; Saegusa et al., 2000; Wilson et al., 2000). Reports on the role of $Ca_V2.1$ channels in pain have been less straightforward with evidence of reduced pain sensitivity in the $Ca_V2.1$ knockout mice (Luvisetto et al., 2006) but hypersensitivity using pharmacological blockade of $Ca_V2.1$ at supraspinal levels (Ebersberger et al., 2004; Knight et al., 2002). In terms of potential adverse effects, $Ca_V2.1^{-/-}$ mice, which die within 3-4 weeks of birth, exhibit ataxia, dystonia, and absence seizures. This phenotype is consistent with human $Ca_V2.1$ loss-of-function mutations which result in episodic ataxia and absence seizures (Pietrobon, 2005). Despite this, the efficacy and safety data of TROX-1 in animal models suggest that an adequate safety window can be obtained with a state-dependent, non-selective Ca_V2 inhibitor (Abbadie et al., 2010). The therapeutic window for a given compound is likely to depend on both its molecular selectivity as well as its degree of state-dependence. Until additional studies are reported for a range of $Ca_V2.2$ inhibitors, the combination of selectivity and state-dependent profiles that best maximize the safety window will remain an open question.

Molecular Pharmacology Fast Forward. Published on December 21, 2011 as DOI: 10.1124/mol.111.075226
This article has not been copyedited and formatted. The final version may differ from this version.

A number of small molecule $Ca_V2.2$ inhibitors have now been reported with various potencies and selectivity profiles (Yamamoto and Takahara, 2009). High affinity $Ca_V1.2$ (L-type) calcium channel inhibitors carry known cardiovascular liabilities and much effort has focused on developing $Ca_V2.2$ inhibitors with selectivity over L-type channels (Abbadie et al., 2010; Zamponi et al., 2009; Zhang et al., 2008). Selectivity against Ca_V3 (T-type) calcium channels and other Ca_V2 subfamily members has also been reported but, in general, have been much more limited (Yamamoto and Takahara, 2009). As shown here, for state-dependent inhibitors, it is important to generate selectivity data in assays producing similar degrees of channel inactivation. Furthermore, a more informative and detailed understanding of inhibitor selectivity profiles can be obtained by looking at potencies across a range of voltages and inactivation levels, particularly for closely related family members where true molecular selectivity may be more difficult to obtain. This is illustrated in the electrophysiological selectivity data for $Ca_V2.1$, $Ca_V2.2$ and $Ca_V2.3$ at -100 mV where TROX-1 appears to be ~30-fold selective over $Ca_V2.1$ channels but, actually, shows no true molecular selectivity.

TROX-1 is an orally available, small molecule $Ca_V2.2$ inhibitor with efficacy in a number of animal models and a demonstrated therapeutic window in animals over cardiovascular and neurological side effects (Abbadie et al., 2010). This paper provides a detailed characterization of the state-dependent and use-dependent properties of TROX-1. The comprehensive selectivity characterization shows that TROX-1 is a state-dependent inhibitor of all members of the Ca_V2 subfamily with similar potency when normalized to the degree of inactivation. Together, these data support the idea that a state-dependent Ca_V2 inhibitor can provide an improved therapeutic window over a relatively state-

Molecular Pharmacology Fast Forward. Published on December 21, 2011 as DOI: 10.1124/mol.111.075226
This article has not been copyedited and formatted. The final version may differ from this version.

independent $Ca_V2.2$ inhibitor, such as ziconotide (Abbadie et al., 2010; Snutch, 2005). Additionally, this paper presents the most comprehensive characterization of a small molecule Cav2 inhibitor to date and should further promote the use of TROX-1 as a benchmark compound. As detailed compound characterizations become available for additional Ca_V2 inhibitors, our understanding of how state-dependence and selectivity influences safety margins and analgesic efficacy will improve. The preclinical profile of TROX-1 suggests a potential future avenue to develop small molecule $Ca_v2.2$ blockers for clinical trials. Ultimately, optimizing state-dependence and selectivity will be essential to realize the full therapeutic potential of targeting $Ca_V2.2$ channels.

Acknowledgements: We thank members of the Ion Channel Department, Merck Research Labs and Dr. Elizabeth Tringham, Zalicus Pharmaceuticals, for helpful discussions.

Authorship Contributions:

Participated in Research Design: AMS, JH, RMB, MMS, SPA, CE, TPS, JLD, GJK and OBM

Conducted Experiments: AMS, JH, RMB, GD, RJH, KSR, MMS, VAW, CE

Contributed new reagents or analytic tools: DP, SBH, CL, JLD

Performed Data analysis: AMS, JH, RMB, GD, RJH, KSR, MMS, VAW, CE, OBM

Wrote or contributed to the writing of the manuscript: AMS, JH, CE, OBM

References

Abbadie C, McManus OB, Sun SY, Bugianesi RM, Dai G, Haedo RJ, Herrington JB, Kaczorowski GJ, Smith MM, Swensen AM, Warren VA, Williams B, Arneric SP, Eduljee C, Snutch TP, Tringham EW, Jochnowitz N, Liang A, Euan MacIntyre D, McGowan E, Mistry S, White VV, Hoyt SB, London C, Lyons KA, Bunting PB, Volksdorf S and Duffy JL (2010) Analgesic effects of a substituted N-triazole oxindole (TROX-1), a state-dependent, voltage-gated calcium channel 2 blocker. *J Pharmacol Exp Ther* **334**(2):545-555.

Bean BP (1984) Nitrendipine block of cardiac calcium channels: high-affinity binding to the inactivated state. *Proc Natl Acad Sci U S A* **81**(20):6388-6392.

Bezprozvanny I, Scheller RH and Tsien RW (1995) Functional impact of syntaxin on gating of N-type and Q-type calcium channels. *Nature* **378**(6557):623-626.

Bourinet E, Soong TW, Sutton K, Slaymaker S, Mathews E, Monteil A, Zamponi GW, Nargeot J and Snutch TP (1999) Splicing of alpha 1A subunit gene generates phenotypic variants of P- and Q-type calcium channels. *Nat Neurosci* **2**(5):407-415.

Cizkova D, Marsala J, Lukacova N, Marsala M, Jergova S, Orendacova J and Yaksh TL (2002) Localization of N-type Ca2+ channels in the rat spinal cord following chronic constrictive nerve injury. *Exp Brain Res FIELD Full Journal Title:Experimental Brain Research* **147**(4):456-463.

Dai G, Haedo RJ, Warren VA, Ratliff KS, Bugianesi RM, Rush A, Williams ME, Herrington J, Smith MM, McManus OB and Swensen AM (2008) A high-

throughput assay for evaluating state dependence and subtype selectivity of Cav2 calcium channel inhibitors. *Assay Drug Dev Technol* **6**(2):195-212.

De Waard M and Campbell KP (1995) Subunit regulation of the neuronal alpha 1A Ca2+ channel expressed in Xenopus oocytes. *J Physiol* **485 (Pt 3)**:619-634.

Ebersberger A, Portz S, Meissner W, Schaible HG and Richter F (2004) Effects of N-, P/Q- and L-type calcium channel blockers on nociceptive neurones of the trigeminal nucleus with input from the dura. *Cephalalgia* **24**(4):250-261.

Evans AR, Nicol GD and Vasko MR (1996) Differential regulation of evoked peptide release by voltage-sensitive calcium channels in rat sensory neurons. *Brain Res* **712**(2):265-273.

Feng ZP, Doering CJ, Winkfein RJ, Beedle AM, Spafford JD and Zamponi GW (2003) Determinants of inhibition of transiently expressed voltage-gated calcium channels by omega-conotoxins GVIA and MVIIA. *J Biol Chem* **278**(22):20171-20178.

Gohil K, Bell JR, Ramachandran J and Miljanich GP (1994) Neuroanatomical distribution of receptors for a novel voltage-sensitive calcium-channel antagonist, SNX-230 (w-conopeptide MVIIC). *Brain Res FIELD Full Journal Title:Brain Research* **653**(1-2):258-266.

Hans M, Urrutia A, Deal C, Brust PF, Stauderman K, Ellis SB, Harpold MM, Johnson EC and Williams ME (1999) Structural elements in domain IV that influence biophysical and pharmacological properties of human alpha1A-containing high-voltage-activated calcium channels. *Biophys J* **76**(3):1384-1400.

Hatakeyama S, Wakamori M, Ino M, Miyamoto N, Takahashi E, Yoshinaga T, Sawada K, Imoto K, Tanaka I, Yoshizawa T, Nishizawa Y, Mori Y, Niidome T and Shoji Si (2001) Differential nociceptive responses in mice lacking the a1B subunit of N-type Ca2+ channels. *NeuroReport FIELD Full Journal Title:NeuroReport* **12**(11):2423-2427.

Kim C, Jun K, Lee T, Kim SS, McEnery MW, Chin H, Kim HL, Park JM, Kim DK, Jung SJ, Kim J and Shin HS (2001) Altered nociceptive response in mice deficient in the alpha(1B) subunit of the voltage-dependent calcium channel. *Mol Cell Neurosci* **18**(2):235-245.

Kiyonaka S, Wakamori M, Miki T, Uriu Y, Nonaka M, Bito H, Beedle AM, Mori E, Hara Y, De Waard M, Kanagawa M, Itakura M, Takahashi M, Campbell KP and Mori Y (2007) RIM1 confers sustained activity and neurotransmitter vesicle anchoring to presynaptic Ca2+ channels. *Nat Neurosci* **10**(6):691-701.

Knight YE, Bartsch T, Kaube H and Goadsby PJ (2002) P/Q-type calcium-channel blockade in the periaqueductal gray facilitates trigeminal nociception: a functional genetic link for migraine? *J Neurosci* **22**(5):RC213.

Luvisetto S, Marinelli S, Panasiti MS, D'Amato FR, Fletcher CF, Pavone F and Pietrobon D (2006) Pain sensitivity in mice lacking the Ca(v)2.1alpha1 subunit of P/Q-type Ca2+ channels. *Neuroscience* **142**(3):823-832.

Malmberg AB and Yaksh TL (1995) Effect of continuous intrathecal infusion of omega-conopeptides, N-type calcium-channel blockers, on behavior and antinociception in the formalin and hot-plate tests in rats. *Pain* **60**(1):83-90.

Matsuda Y, Saegusa H, Zong S, Noda T and Tanabe T (2001) Mice lacking Ca(v)2.3 (alpha1E) calcium channel exhibit hyperglycemia. *Biochem Biophys Res Commun* **289**(4):791-795.

McDonough SI and Bean BP (1998) Mibefradil inhibition of T-type calcium channels in cerebellar purkinje neurons. *Mol Pharmacol* **54**(6):1080-1087.

McGivern JG and McDonough SI (2004) Voltage-gated calcium channels as targets for the treatment of chronic pain. *Curr Drug Targets CNS Neurol Disord* **3**(6):457-478.

Miljanich GP (2004) Ziconotide: neuronal calcium channel blocker for treating severe chronic pain. *Curr Med Chem* **11**(23):3029-3040.

Perier F, Radeke CM and Vandenberg CA (1994) Primary structure and characterization of a small-conductance inwardly rectifying potassium channel from human hippocampus. *Proc Natl Acad Sci U S A* **91**(13):6240-6244.

Pietrobon D (2005) Function and dysfunction of synaptic calcium channels: insights from mouse models. *Curr Opin Neurobiol* **15**(3):257-265.

Saegusa H, Kurihara T, Zong S, Kazuno A, Matsuda Y, Nonaka T, Han W, Toriyama H and Tanabe T (2001) Suppression of inflammatory and neuropathic pain symptoms in mice lacking the N-type Ca2+ channel. *Embo J* **20**(10):2349-2356.

Saegusa H, Kurihara T, Zong S, Minowa O, Kazuno A, Han W, Matsuda Y, Yamanaka H, Osanai M, Noda T and Tanabe T (2000) Altered pain responses in mice lacking alpha 1E subunit of the voltage-dependent Ca2+ channel. *Proc Natl Acad Sci U S A* **97**(11):6132-6137.

Scott DA, Wright CE and Angus JA (2002) Actions of intrathecal omega-conotoxins CVID, GVIA, MVIIA, and morphine in acute and neuropathic pain in the rat. *Eur J Pharmacol* **451**(3):279-286.

Snutch TP (2005) Targeting chronic and neuropathic pain: the N-type calcium channel comes of age. *NeuroRx* **2**(4):662-670.

Staats PS, Yearwood T, Charapata SG, Presley RW, Wallace MS, Byas-Smith M, Fisher R, Bryce DA, Mangieri EA, Luther RR, Mayo M, McGuire D and Ellis D (2004) Intrathecal ziconotide in the treatment of refractory pain in patients with cancer or AIDS: a randomized controlled trial. *Jama* **291**(1):63-70.

Stocker JW, Nadasdi L, Aldrich RW and Tsien RW (1997) Preferential interaction of omega-conotoxins with inactivated N-type Ca2+ channels. *J Neurosci* **17**(9):3002-3013.

Thaler C, Gray AC and Lipscombe D (2004) Cumulative inactivation of N-type CaV2.2 calcium channels modified by alternative splicing. *Proc Natl Acad Sci U S A* **101**(15):5675-5679.

Westenbroek RE, Hoskins L and Catterall WA (1998) Localization of Ca2+ channel subtypes on rat spinal motor neurons, interneurons, and nerve terminals. *J Neurosci* **18**(16):6319-6330.

Williams ME, Brust PF, Feldman DH, Patthi S, Simerson S, Maroufi A, McCue AF, Velicelebi G, Ellis SB and Harpold MM (1992) Structure and functional expression of an omega-conotoxin-sensitive human N-type calcium channel. *Science* **257**(5068):389-395.

Williams ME, Marubio LM, Deal CR, Hans M, Brust PF, Philipson LH, Miller RJ, Johnson EC, Harpold MM and Ellis SB (1994) Structure and functional characterization of neuronal alpha 1E calcium channel subtypes. *J Biol Chem* **269**(35):22347-22357.

Wilson SM, Toth PT, Oh SB, Gillard SE, Volsen S, Ren D, Philipson LH, Lee EC, Fletcher CF, Tessarollo L, Copeland NG, Jenkins NA and Miller RJ (2000) The status of voltage-dependent calcium channels in alpha 1E knock-out mice. *J Neurosci* **20**(23):8566-8571.

Winquist RJ, Pan JQ and Gribkoff VK (2005) Use-dependent blockade of Cav2.2 voltage-gated calcium channels for neuropathic pain. *Biochem Pharmacol* **70**(4):489-499.

Yamamoto T and Takahara A (2009) Recent updates of N-type calcium channel blockers with therapeutic potential for neuropathic pain and stroke. *Curr Top Med Chem* **9**(4):377-395.

Zamponi GW, Feng ZP, Zhang L, Pajouhesh H, Ding Y, Belardetti F, Pajouhesh H, Dolphin D, Mitscher LA and Snutch TP (2009) Scaffold-based design and synthesis of potent N-type calcium channel blockers. *Bioorg Med Chem Lett* **19**(22):6467-6472.

Zhang S, Su R, Zhang C, Liu X, Li J and Zheng J (2008) C101, a novel 4-amino-piperidine derivative selectively blocks N-type calcium channels. *European Journal of Pharmacology* **587**(1-3):42.

Zhong H, Yokoyama CT, Scheuer T and Catterall WA (1999) Reciprocal regulation of P/Q-type Ca2+ channels by SNAP-25, syntaxin and synaptotagmin. *Nat Neurosci* **2**(11):939-941.

Footnotes Present addresses of authors:

A.M.S.
Abbott Neuroscience
100 Abbott Park Rd.
Abbott Park, IL 60064

J.H.
Biochemical Pharmacology | Small Molecule Drug Discovery
Genentech Research & Early Development
Genentech, Inc.
1 DNA Way
South San Francisco, CA 94080

R.J.H.
Nanion Technologies Inc.
675 US Highway One
North Brunswick, NJ 08902

K.S.R.
Pain/Migraine DHT
Eli Lilly and Company
Indianapolis, Indiana 46285

V.A.W.
Koltan Pharmaceuticals
300 George St, Suite 530
New Haven, CT 06511

S.P.A.
Pain/Migraine DHT
Eli Lilly and Company
Indianapolis, Indiana 46285

G.J.K.
Kanalis Consulting
5 Ashbrook Drive
Edison, New Jersey 08820

O.B.M.
Johns Hopkins Ion Channel Center
High Throughput Biology Center
Department of Neuroscience
Johns Hopkins Medical School
733 North Broadway
Baltimore, MD 21205

Molecular Pharmacology Fast Forward. Published on December 21, 2011 as DOI: 10.1124/mol.111.075226
This article has not been copyedited and formatted. The final version may differ from this version.

Financial Disclosure Information

A.M.S., J.H., R.M.B., G.D., R.J.H., K.S.R., M.M.S., V.A.W., S.B.H., C.L., J.L.D., G.J.K. and O.B.M. are present or former employees of Merck Research Laboratories and may hold stock or stock options in Merck & Co. S.P.A., C.E., D.P. and T.P.S. are present or former employees in Zalicus Pharmaceuticals and may hold stock or stock options in Zalicus Pharmaceuticals.

Andrew M. Swensen, James Herrington - Contributed equally to this work

Molecular Pharmacology Fast Forward. Published on December 21, 2011 as DOI: 10.1124/mol.111.075226
This article has not been copyedited and formatted. The final version may differ from this version.

Figure Legends

Figure 1. Characterization of bMHN-4 $Ca_V2.2$ cell line. (A) The bMHN-4 $Ca_V2.2$ cell line (n=14 cells) showed improved current stability relative to the 2H8 cell line (n=7 cells). Peak current amplitudes were measured on PatchXpress every 15 seconds in response to a 50 ms depolarizing step to +10 mV from a holding potential of –90 mV. (B) Characterization of the voltage-dependence of bMHN-4 currents. The current vs voltage relationship shows that the peak current amplitudes were elicited near +5 mV (n=5 cells). Activation (n=4 cells) and inactivation (n=5 cells) data were fit with a Boltzmann relationship (see Materials and Methods for protocol details). Best fits to the data yielded a half activation voltage of +4 mV with a slope factor of 9.1 and a half inactivation voltage of -80 mV with a slope factor of -11.5. Data are shown as mean ± S.E.M.. (C) Example illustrating the inhibition of current from the bMHN-4 cell line by 500 nM of the $Ca_V2.2$-selective peptidyl inhibitor, ω-conotoxin GVIA. Current was elicited in response to a 20 ms step to +10 mV from a holding potential of -110 mV.

Figure 2. TROX-1 inhibition of $Ca_V2.2$ current assessed by manual electrophysiology. (A) Chemical structure of the substituted N-triazole oxindole, TROX-1. (B, C) Representative current traces illustrating the inhibition of $Ca_V2.2$ current by 300 nM TROX-1 utilizing the depolarized (B) and hyperpolarized (C) electrophysiological protocols. (D) Concentration-response data for TROX-1 under depolarized (n=3 cells) and hyperpolarized (n=3-4 cells) conditions. Voltage protocol details are given in the text. Solid line is a fit of the Hill equation to the data; IC_{50} value from the fit is given in the text.

Molecular Pharmacology Fast Forward. Published on December 21, 2011 as DOI: 10.1124/mol.111.075226
This article has not been copyedited and formatted. The final version may differ from this version.

Figure 3. State-dependence of TROX-1 inhibition of $Ca_V2.2$ channels measured by automated electrophysiology. (A) Plot of the peak inward current versus time for a cell (bMHN-4) recorded on the PatchXpress™ (left). The solid bars represent when TROX-1 was present in the well at the concentrations shown. The membrane potential was stepped to +10 mV every 15 seconds from a holding potential of -70 mV. Representative leakage-subtracted currents prior to and after adding 0.3 uM and 3 uM TROX-1 are shown at right. (B) Plot of peak inward current versus time (left) for a different cell under identical conditions as in A except that the holding potential was -110 mV. Representative leakage-subtracted currents prior to and after adding 3 uM and 10 uM TROX-1 are shown at right. The peak tail current has been truncated for scaling purposes. (C) Plot of the average percent inhibition of peak inward $Ca_V2.2$ current versus the concentration of TROX-1. The solid lines are fits of the Hill equation to the data; IC_{50} values from the fits are given in the text. For -70 mV and -90 mV, n=6 for each data point. For -110 mV data, n=6 for 1 uM and 30 uM and n=8 for 3 uM and 10 uM.

Figure 4. Use-dependent inhibition of $Ca_V2.2$ channels by TROX-1. (A) Representative $Ca_V2.2$ currents recorded on the PatchXpress prior to and after application of 3 uM TROX-1. CBK cells were voltage clamped at –60 mV and trains of twenty 25 msec pulses to +20 mV were applied at a frequency of 2 Hz every 5 minutes. Shown are the currents in response to Pulse 1 (top) and Pulse 20 (bottom) of the train. (B) Plot of the average percent inhibition of peak inward $Ca_V2.2$ current at Pulse 1 and Pulse 20 versus the concentration of TROX-1. Solid lines are fits of the Hill equation to the data. IC_{50}

values from the fits are given in the text. For each data point n=5. (C) Plots of peak current (left) and end current amplitude (right) versus sweep number prior to (open symbols) and following application of 3 μM TROX-1 (closed symbols) for the recording shown in (A).

Figure 5. Comparison of TROX-1 inhibition of $Ca_V2.1$, $Ca_V2.2$, and $Ca_V2.3$ current assessed by manual electrophysiology. Utilizing the depolarized voltage format where $Ca_V2.1$, $Ca_V2.2$ and $Ca_V2.3$ channels were similarly inactivated, TROX-1 inhibited all three Ca_V2 subfamily members with a similar potency. Although TROX-1 displayed state-dependent inhibition of all three Ca_V2 subfamily members, TROX-1 inhibition measured utilizing the hyperpolarized voltage format was less potent for $Ca_V2.1$ than that observed for $Ca_V2.2$ and $Ca_V2.3$. Voltage protocol details are given in the text. Solid lines are fits of the Hill equation to the data; IC_{50} values from the fits are given in the text. For the depolarized voltage format, n=6, 9 and 7 cells for $Ca_V2.1$, $Ca_V2.2$ and $Ca_V2.3$, respectively. For the hyperpolarized voltage format, n=5, 5 and 9 cells for $Ca_V2.1$, $Ca_V2.2$, and $Ca_V2.3$, respectively.

Figure 6. Selectivity and state-dependent inhibition of $Ca_V2.1$, $Ca_V2.2$ and $Ca_V2.3$ channels in a calcium-influx assay. Top Panels: Data from a row of twenty four wells in a 384 well assay plate showing calcium influx under either hyperpolarized (A, 4 mM K^+ pre-incubation) or depolarized (B, 14 mM K^+ pre-incubation) conditions followed by a 140 mM K^+ addition (1:1) to depolarize cells and open channels. The leftmost two wells in each row contained 10 μM of a nonselective Cav2.x blocker, the next two wells from

the left contain control buffer, and the following wells contain increasing concentrations of TROX-1 in a ten point titration format in duplicate from 1 nM to 30 μM. Bottom Panels: Analysis of TROX-1 concentration-response data for each experiment under hyperpolarized (A) or depolarized (B) conditions. Data are reported as the mean ± S.E.M (n=4). Solid lines are fits of the Hill equation to the data; IC_{50} values from the fits are given in the text.

Figure 7. Relationship between TROX-1 potency and calcium channel inactivation for $Ca_V2.1$, $Ca_V2.2$ and $Ca_V2.3$ channels in a calcium-influx assay. (A, B and C) Plots of TROX-1 IC_{50} values (colored symbols; n=4 experiments) and peak fluorescent signal (black squares; one experiment in quadruplicate) vs the pre-incubation external potassium concentration for $Ca_V2.1$ (A), $Ca_V2.2$ (B) and $Ca_V2.3$ (C). (D) Plot of TROX-1 IC_{50} values vs the fractional reduction in the peak calcium signal for $Ca_V2.1$ (blue), $Ca_V2.2$ (red) and $Ca_V2.3$ (green).

Molecular Pharmacology Fast Forward. Published on December 21, 2011 as DOI: 10.1124/mol.111.075226
This article has not been copyedited and formatted. The final version may differ from this version.

Tables

TABLE 1. Comparison of current expression in the CBK, 2H8, and bMHN-4 $Ca_V2.2$ stable cell lines as measured by automated electrophysiology. Peak current amplitudes were measured on PatchXpress in response to a 50 ms depolarizing step to +10 mV from a holding potential of –90 mV. Data are reported as mean ± S.E.M.

Cell Line	Current at +10 mV	n
CBK	1.6 ± 0.6 nA	8
2H8	5.6 ± 0.7 nA	21
bMHN-4	2.2 ± 0.5 nA	14

Figure 1

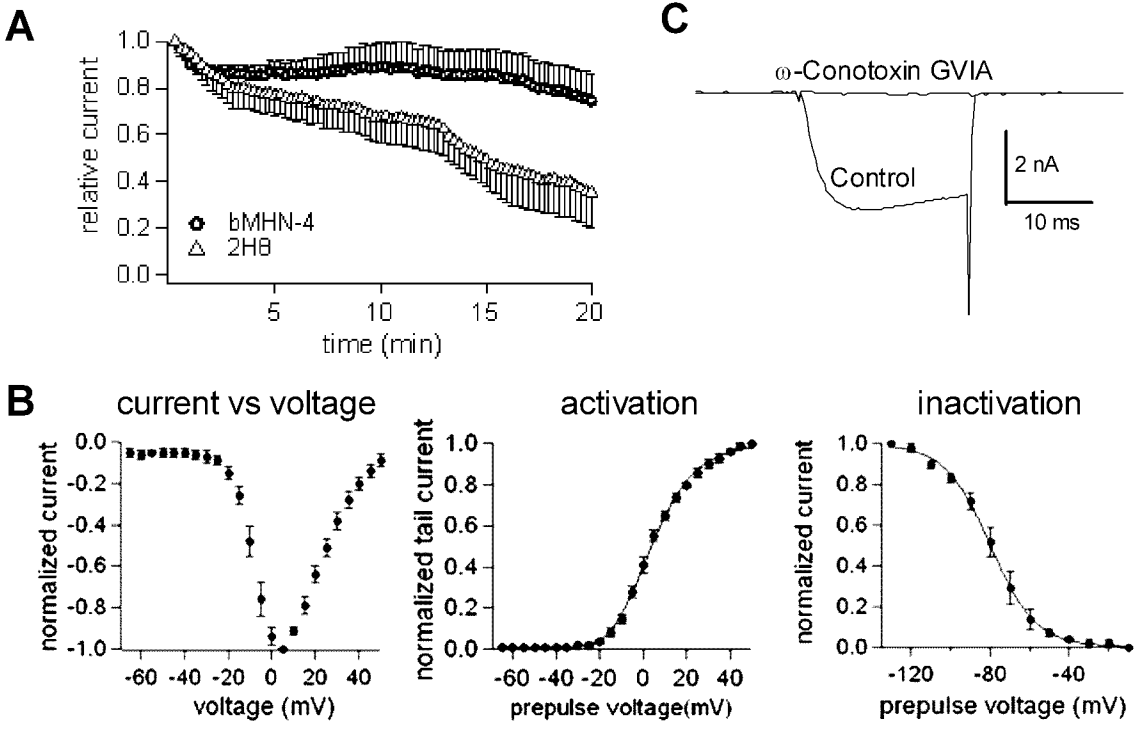
A
relative current
1.0
0.8
0.6
0.4
0.2
0.0
bMHN-4
2H8
5
10
15
20
time (min)
C
ω-Conotoxin GVIA
Control
2 nA
10 ms
B
current vs voltage
normalized current
0.0
-0.2
-0.4
-0.6
-0.8
-1.0
-60 -40 -20 0 20 40
voltage (mV)
activation
normalized tail current
1.0
0.8
0.6
0.4
0.2
0.0
-60 -40 -20 0 20 40
prepulse voltage(mV)
inactivation
normalized current
1.0
0.8
0.6
0.4
0.2
0.0
-120 -80 -40
prepulse voltage (mV)

Figure 2

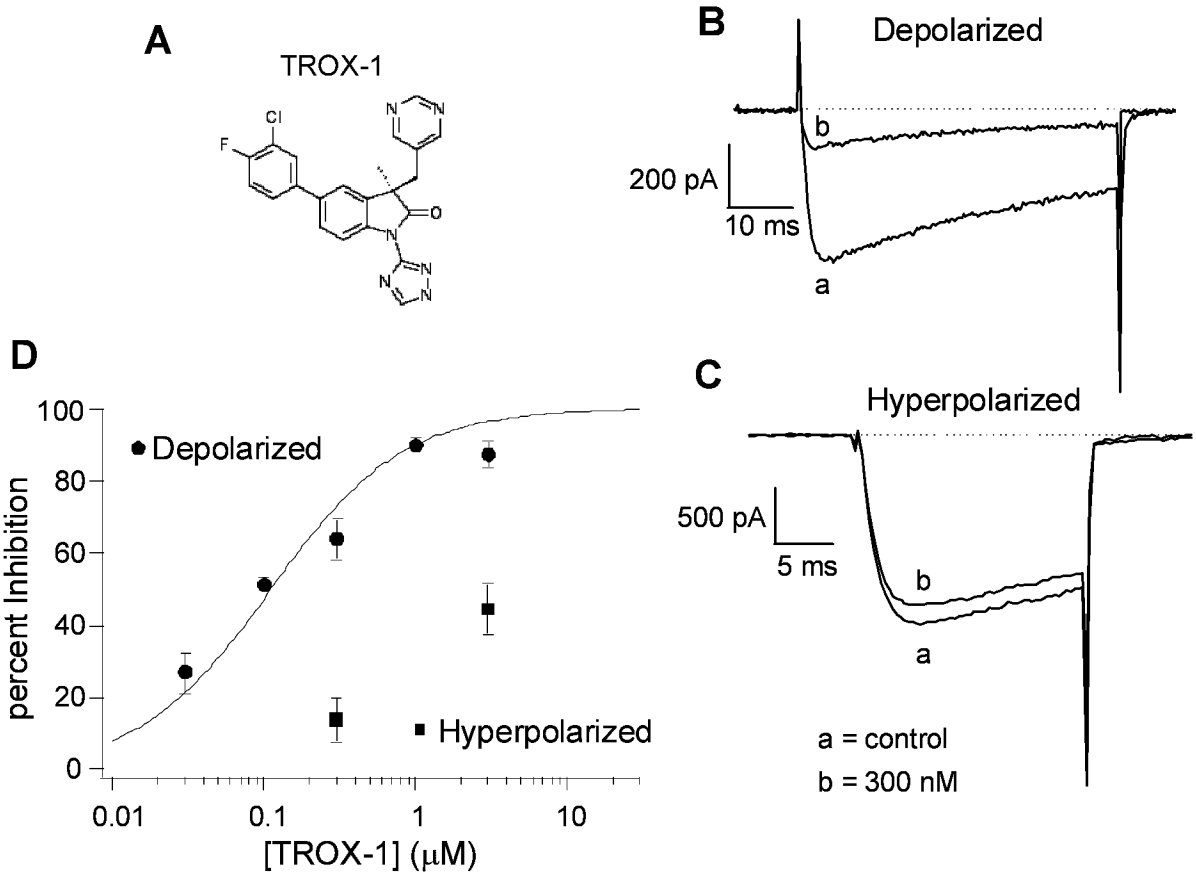
A
TROX-1
Cl
F
N
N
O
N
N
N
N
B
Depolarized
b
200 pA
10 ms
a
C
Hyperpolarized
500 pA
5 ms
b
a
a = control
b = 300 nM
D
percent Inhibition
100
80
60
40
20
0
Depolarized
Hyperpolarized
0.01
0.1
1
10
[TROX-1] (μM)

Figure 3

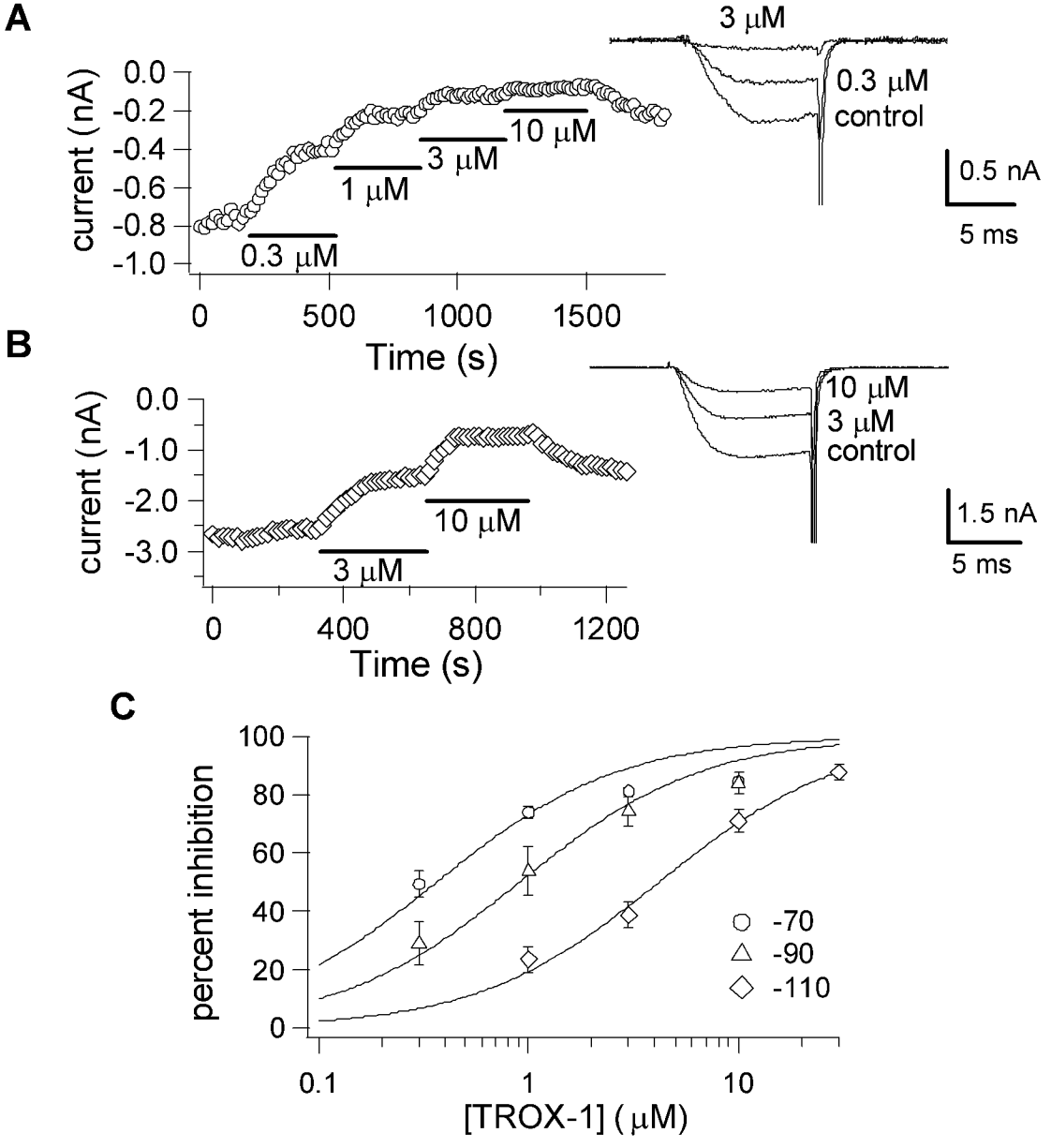
A
current (nA)
0.0
-0.2
-0.4
-0.6
-0.8
-1.0
0.3 μM
1 μM
3 μM
10 μM
0
500
1000
1500
Time (s)
3 μM
0.3 μM
control
0.5 nA
5 ms
B
current (nA)
0.0
-1.0
-2.0
-3.0
3 μM
10 μM
0
400
800
1200
Time (s)
10 μM
3 μM
control
1.5 nA
5 ms
C
percent inhibition
100
80
60
40
20
0
0.1
1
10
[TROX-1] (μM)
-70
-90
-110

Figure 4

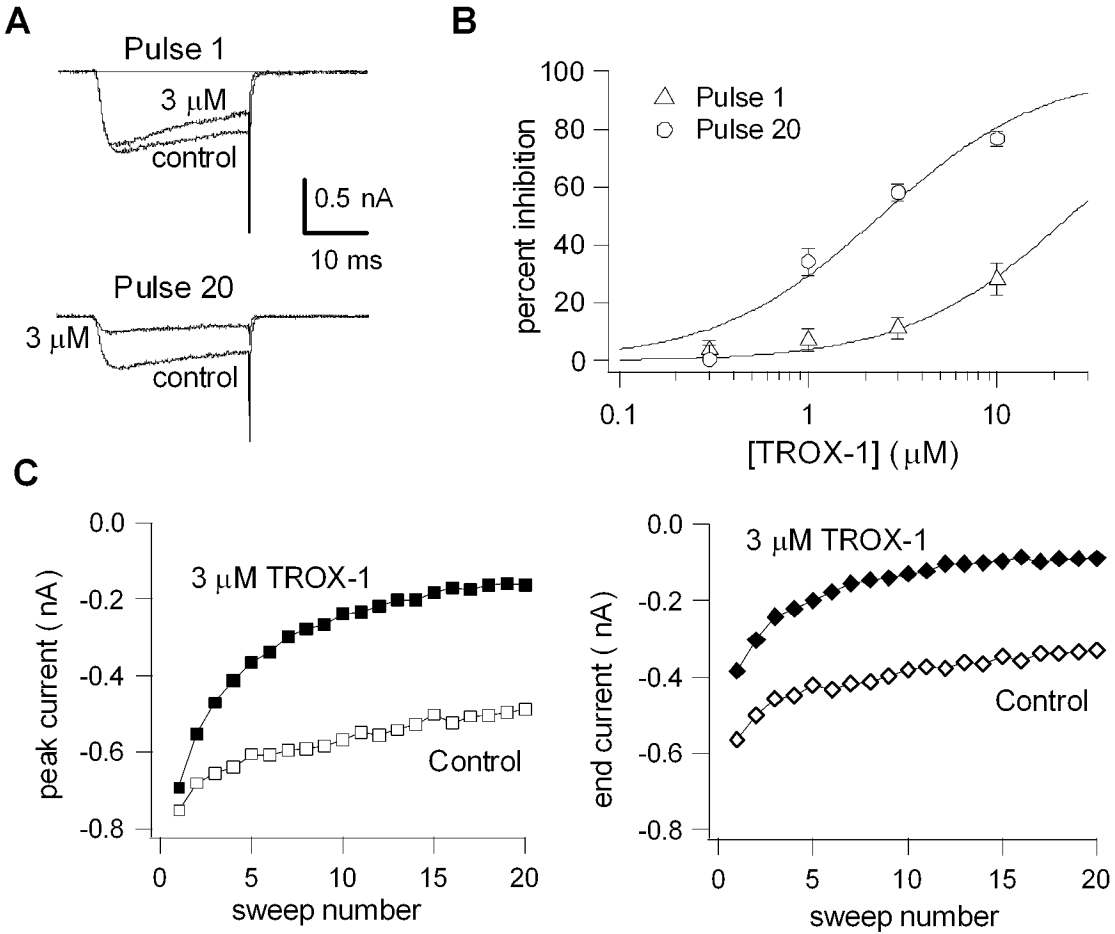
A
Pulse 1
3 μM
control
0.5 nA
10 ms
Pulse 20
3 μM
control
B
Pulse 1
Pulse 20
percent inhibition
100
80
60
40
20
0
0.1
1
10
[TROX-1] (μM)
C
3 μM TROX-1
Control
peak current (nA)
0.0
-0.2
-0.4
-0.6
-0.8
0
5
10
15
20
sweep number
3 μM TROX-1
Control
end current (nA)
0.0
-0.2
-0.4
-0.6
-0.8
0
5
10
15
20
sweep number

Figure 5

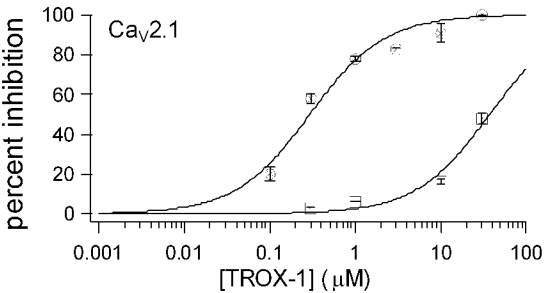
Ca$_V$2.1
percent inhibition
100
80
60
40
20
0
0.001
0.01
0.1
1
10
100
[TROX-1] (μM)

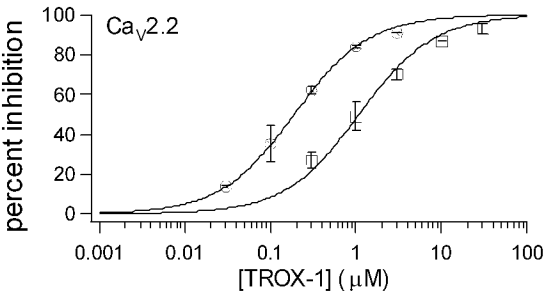
Ca$_V$2.2
percent inhibition
100
80
60
40
20
0
0.001
0.01
0.1
1
10
100
[TROX-1] (μM)

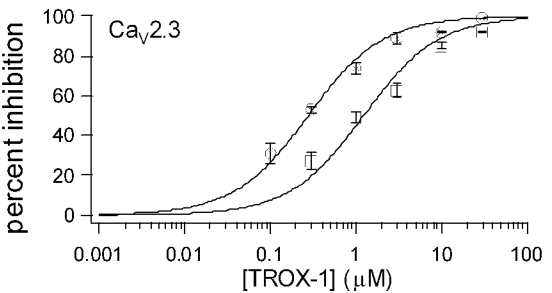
Ca$_V$2.3
percent inhibition
100
80
60
40
20
0
0.001
0.01
0.1
1
10
100
[TROX-1] (μM)

Figure 6

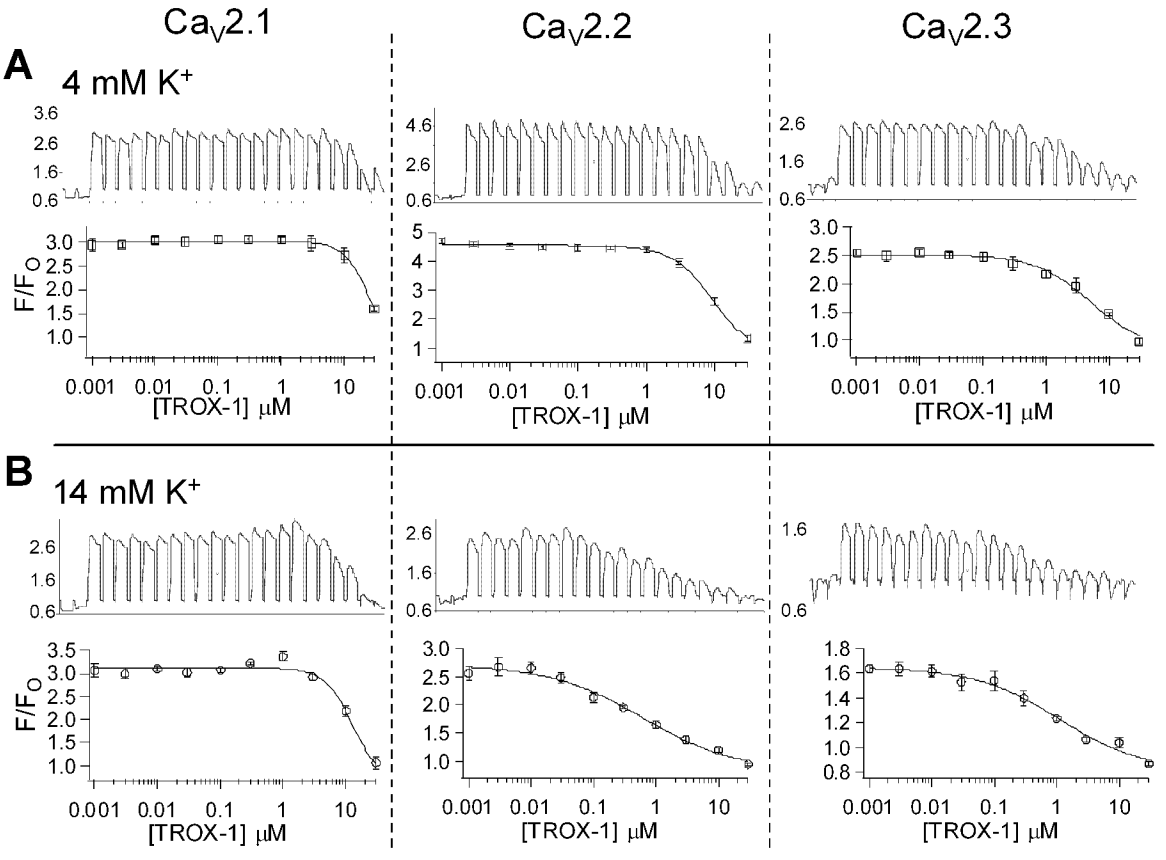
Ca$_V$2.1
Ca$_V$2.2
Ca$_V$2.3
A
4 mM K$^+$
3.6
2.6
1.6
0.6
4.6
2.6
0.6
2.6
1.6
0.6
F/F$_O$
3.0
2.5
2.0
1.5
1.0
5
4
3
2
1
3.0
2.5
2.0
1.5
1.0
0.001 0.01 0.1 1 10
[TROX-1] μM
B
14 mM K$^+$
2.6
1.6
0.6
2.6
1.6
0.6
1.6
0.6
F/F$_O$
3.5
3.0
2.5
2.0
1.5
1.0
3.0
2.5
2.0
1.5
1.0
1.8
1.6
1.4
1.2
1.0
0.8
0.001 0.01 0.1 1 10
[TROX-1] μM

Figure 7

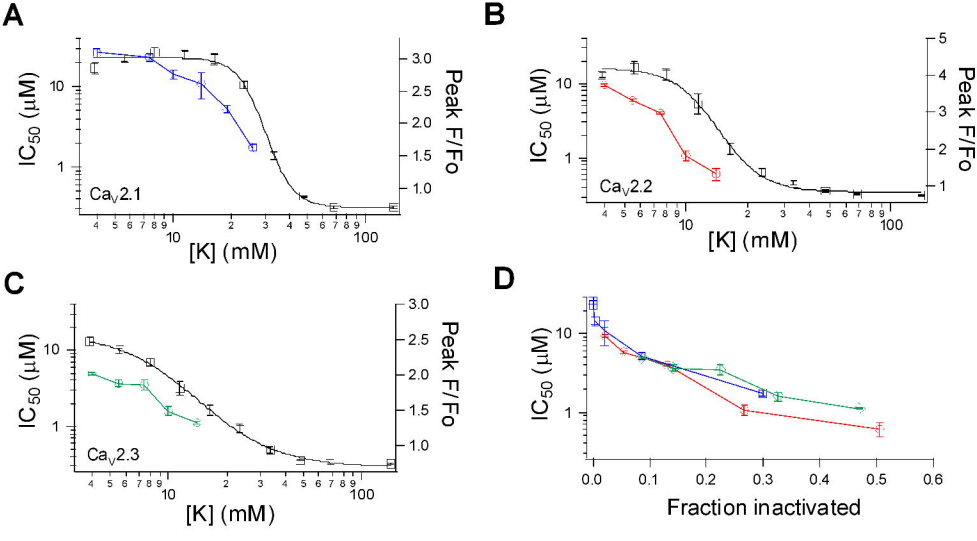
A
B
C
D
IC50 (μM)
Peak F/Fo
[K] (mM)
CaV2.1
CaV2.2
CaV2.3
Fraction inactivated